Photoinduced Structural Dynamics in Laser-Heated Nanomaterials of Various Shapes and Sizes

Pyng Yu,[†] Jau Tang,*[,‡] and Sheng-Hsien Lin*[,§,||]

Department of Chemistry, National Taiwan University, Taipei, Taiwan, Research Center for Applied Sciences, Academia Sinica, Taiwan, Institute of Atomic and Molecular Sciences, Academia Sinica, Taipei, Taiwan, Institute of Molecular Science and Department of Applied Chemistry, National Chiao-Tung University, Hsinchu, Taiwan

Received: July 23, 2008; Revised Manuscript Received: September 4, 2008

We examined photoinduced ultrafast structural dynamics such as coherent acoustic waves in many shapes of fcc metallic nanomaterials. Experimental data of nanosized thin films, prisms, spheres, rods, disks and pyramids from transient optical absorption/reflectance measurements were analyzed based on a combined Fermi-Pasta-Ulam model and two-temperature model. This work elucidates the structural dynamics induced by femtosecond laser heating, its size and shape effects on the period and phase of the excited acoustic phonon modes.

Introduction

Generation of a transient acoustic wave in condensed matter by an optical pulse, known as the optoacoustic effect, has been a longstanding research subject to many scientists.[1,2] It has been more hotly pursued recently as a result of advances in fabrication of nanosize materials. The laser heating effects by a short laser pulse on bulk-size metals and semiconductors have been a subject of extensive research over the past two decades. Understanding the ultrafast dynamics of hot charged carriers and their interactions with phonons and the subsequent thermal relaxation are important to elucidate many laser-induced phenomena.[3−9] More recently, laser heating of nanostructured materials of various shapes and their potential application in medical treatment have generated widespread interest among researchers. In metal nanomaterials, the surface plasmon resonance (SPR) band is sensitive to the size and shape of the particles and the dielectric environment.[10] Laser heating with a femtosecond pulse induces lattice vibration and a periodic shift of the SPR band position or bandwidth,[11,12] which results in modulations in the transient absorption intensity at the probed wavelength. Accordingly, transient acoustic vibration in thin films,[13,14] spherical nanoparticles,[10] and nanoprisms[12,15,16] and nanorods[17] has been mostly investigated by transient absorption/reflection techniques. Other than transient optical absorption/reflectivity, oscillations have been observed by time-resolved X-ray diffraction[18,19] and electron diffraction.[20]

FPU−TTM Model. In most phenomenological treatments of acoustic wave excitation, one assumes the whole slab or nanoparticle behaves as a damped oscillator. Recently, a combined FPU−TTM model[21] was employed to explain the peak shift in ultrafast electron diffraction rings of a laser-heated polycrystalline aluminum film. This more realistic model combines the Fermi−Pasta−Ulam (FPU) model describing impulse-induced structural dynamics and the two-temperature model (TTM)[22,23] describing laser heating and heat transfer of conduction electrons and phonons. In this work, we extend this model to provide a platform for analyzing transient optical absorption data of gold and silver nanomaterials of various shapes and sizes. According to this model, the heat transfer in a metal slab or nanoparticle involves two subsystems, mobile electrons and phonon bath, governed by the following 3-D rate equation,

$$C_e(T)\frac{\partial}{\partial t}T_1(\mathbf{r},t) = \nabla\cdot(\kappa_e\nabla T_1(\mathbf{r},t)) - g(T_1(\mathbf{r},t) - T_2(\mathbf{r},t)) + S(\mathbf{r},t)$$

$$C_2\frac{\partial}{\partial t}T_2(\mathbf{r},t) = \kappa_L\nabla^2 T_2(\mathbf{r},t) - g(T_2(\mathbf{r},t) - T_1(\mathbf{r},t)) - h(T_2(\mathbf{r},t) - T_0) \quad (1a)$$

where $T_1(\mathbf{r}, t)$ and $T_2(\mathbf{r}, t)$ describe electron and phonon temperatures at a position vector, $\mathbf{r}$, and at a time, t, respectively. If one is primarily interested in short-time heat transfer, the heat conduction by phonons (the term involving κ_L) and thermal relaxation to heat bath temperature T_0 (the term involving h) can be neglected. Assuming the incident laser is along the z-axis, the heat source term can be given by

$$S(\mathbf{r},t) = \exp(-4\ln 2\times(t-\tau_0)^2/\tau_p^2)\sqrt{4\ln 2/\pi}\,F_0(1-R)/[\tau_p\xi_L(1-\exp(-L/\xi_L))] \quad (1b)$$

where R is the surface optical reflectivity at the given laser wavelength, L is the substrate thickness traveled by light, F_0 is the fluence of the incident laser, ξ_L the optical penetration depth, and τ_0 and τ_p in the time profile are the delay time and the full width at half-maximum (fwhm) of the laser pulse. The coupling factor, g, describes electron−phonon interactions. For electrons, one has the heat capacity as $C_e = C_1T_1$ and heat conductivity as K_eT_1/T_2. The phonon thermal conductivity, κ_L, can be neglected here. The initial conditions for the electron and lattice subsystems are assumed to be at $T_1(0) = T_2(0) = T_0 = 300$ K.

Here, we extend the usual 1-D FPU chain model to a 3-D periodic atomic array, assuming each atom with an index, n, is coupled to each of its nearest neighbors (index j) by a spring with an anharmonic potential, $m\omega^2(\mathbf{r}_n - \mathbf{r}_j)^2/2 + \alpha\, m\omega^2(\mathbf{r}_n - \mathbf{r}_j)^3/$

* Corresponding authors. E-mails: (J.T.) jautang@gate.sinica.edu.tw, (S.-H.L.) hcshaw@po.iams.sinica.edu.tw.
[†] National Taiwan University.
[‡] Research Center for Applied Sciences, Academia Sinica.
[§] Institute of Atomic and Molecular Sciences, Academia Sinica.
[||] National Chiao-Tung University.

10.1021/jp806498y CCC: $40.75
Published on Web 10/15/2008

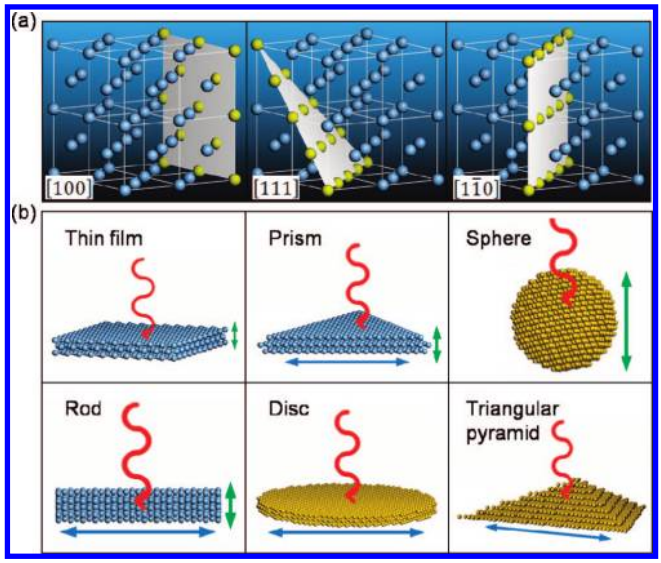

Figure 1. (a) 3-D atomic array in fcc structure, showing [100], [111], and [1$\bar{1}$0] planes. (b) Various shapes of laser-heated nanomaterials to be analyzed in this work.

TABLE 1: Relevant Parameters of Silver and Gold[24−29]

	silver	gold
mass, m	17.92×10^{-26} kg	32.72×10^{-26} kg
sound velocity, $v_S = \omega l$	3650 m/s	3240 m/s
Hook constant, $m\omega^2$	28.58 kg/s^2	41.41 kg/s^2
interatomic distance, l	2.89×10^{-10} m	2.88×10^{-10} m
electronic specific-heat coefficient, C_1	65.0 J/m^3 K^2	71.0 J/m^3 K^2
lattice heat capacity, C_2	2.0×10^6 J/m^3 K	2.5×10^6 J/m^3 K
electron−phonon coupling parameter, g	3.5×10^{16} W/m^3 K	2.1×10^{16} W/m^3 K
optical absorption depth, ξ_l	24.0 nm	16.3 nm
optical reflectivity at 790 nm, R	93%	93%
electron Grüneisen parameter, $\gamma_{2,G}$	1.2	1.6
phonon Grüneisen parameter, $\gamma_{1,G}$	2.4	3.0
electron thermal conductivity, K_e	418 W/m K	318 W/m K
thermal linear expansion, β	1.9×10^{-5}	1.4×10^{-5}

3, where α is the anharmonic factor that is related to the linear thermal expansion coefficient β by $\beta = \alpha k_B/m\omega^2 l$. For each nonboundary atom with fcc structure, shown in Figure 1, there are 12 nearest-neighboring atoms. The equation of motion for an atom at the position $\mathbf{r}_n$ and momentum $\mathbf{p}_n$ is given by

$$\frac{\mathrm{d}}{\mathrm{d}t}\mathbf{r}_n = \frac{\mathbf{p}_n}{m}$$
$$\frac{\mathrm{d}}{\mathrm{d}t}\mathbf{p}_n = \mathbf{F}_n(t) - \gamma\mathbf{p}_n - \nabla U_n \qquad (2)$$

where γ is the frictional coefficient and U_n is the anharmonic potential for that atom. The impulsive force at the nth atomic site along the k-axis is related to the local temperature change by $F_{n,k}(t) = -\gamma_{2,G}l^2C_2(T_2(\mathbf{r}_n, t) - T_0) - \gamma_{1,G}l^2C_1T_1(\mathbf{r}_n, t)(T_1(\mathbf{r}_n, t) - T_0)$, where $T_1(\mathbf{r}_n, t)$ is the electron temperature, $T_2(\mathbf{r}_n, t)$ is the phonon temperature at the nth position and T_0 is the heat bath temperature, $\gamma_{2,G}$ is the phonon Grüneisen parameter, and $\gamma_{1,G}$ is the electron Grüneisen parameter. Listed in Table 1 are the relevant FPU−TTM parameters for gold and silver with reference sources.[24−29] The Hook constant listed there was chosen to produce the correct sound speed for a reduced 1-D model with atoms in closest contact. To obtain the correct sound speed in full treatment of a 3-D fcc lattice, the value needs to be doubled. The Runge−Kutta method was used to obtain a numerical solution of the spatial and temporal behavior of these dynamic variables.

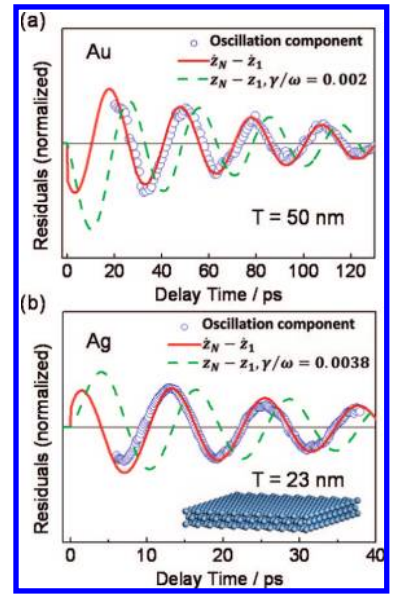

Figure 2. (a) The change of transient reflectance (open circle) of a 50-nm-thick gold film and the simulated result using $N = 168$ (red line) based on FPU−TTM. (b) The transient absorption profile (open circle) of a 23-nm-thick silver film and the simulated result using $N = 77$ (red line).

Analyses of the Experimental Data and Discussion. Now we proceed to analyze some experimental data of nanomaterials with six different sample shapes (Figure 1b) measured by others, including our own (silver nanoprisms and gold nanospheres). We first consider a thin film using 1-D FPT−TTM, where the laser beam is perpendicular to the film surface.[21] In Figure 2a, the transient reflectance data of a gold film with thickness of 50 nm (extracted from Figure 4 in the work of Wang and Guo[13]) is illustrated, in comparison with our model simulation based on FPU−TTM. The result shows excellent agreement with the time derivative of the film thickness, that is, $\dot{z}_N(t) - \dot{z}_1(t)$. On the basis of the well-known dielectric relaxation mechanism, each atom behaves as a damped harmonic oscillator with a frictional force linearly proportional to its velocity and the Hooke restoring force proportional to its displacement from the equilibrium position. The dielectric absorption represents the energy loss caused by the frictional force and is proportional to the velocity of an atom. Therefore, the best fit we obtained in Figure 2a is proportional to the time derivative of the film thickness, that is, $\dot{z}_N(t) - \dot{z}_1(t)$. Shown in Figure 2b is the transient absorption data of a 23-nm-thick silver film (extracted from Figure 3a in the report by Del Fatti and co-workers[14]). The experimental curve agrees with $\dot{z}_N(t) - \dot{z}_1(t)$, which has a 180-degree phase shift as compared to the previous example in Figure 2a, due to the difference in the measurement method. For gold films, changes of transient reflectance were detected, but for silver films, absorption changes were measured. Our simulated curves were obtained with only two adjustable parameters (i.e., the amplitude and the exponential damping rate), and they reproduce experimental oscillation periods and phases. This result is consistent with the longitudinal sound velocity of 3650 m/s for silver. The frequency and damping time constant were found to be 2.61 cm^{-1} (12.77 ps) and 0.82 cm^{-1} (40.8 ps), respectively.

In the second example, we analyzed our own experimental data of nanoprisms. The pump and probe wavelength was set at 575 nm. The deduced oscillations from the transient absorp-

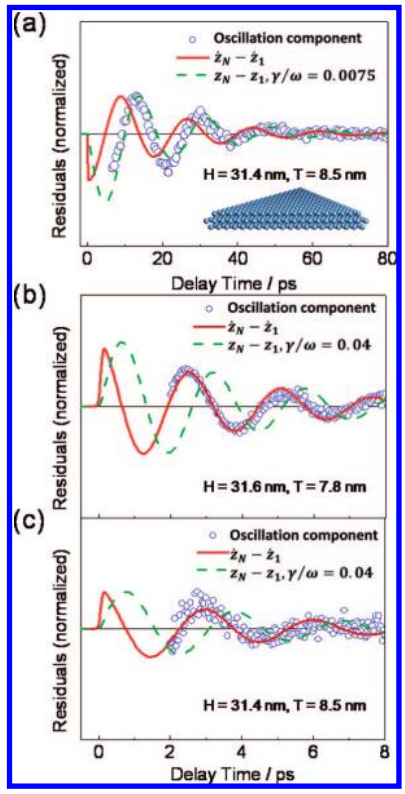

Figure 3. (a) The change of transient absorption of silver nanoprisms (open circle) with a bisector height of 31.4 nm. The long-time slow oscillation period is equal to the bisector height. (b) The observed short-time fast oscillations caused by sound wave propagation perpendicular to the film surface. $N = 16$ was used. (c) The observed short-time fast oscillations for a thicker nanoprism, corresponding to $N = 19$.

tion trace (Figure 3a) is in good agreement with the 1-D FPU−TTM model calculation using $z_N(t) - z_1(t)$. The period is equal to twice the bisector height divided by the sound speed.

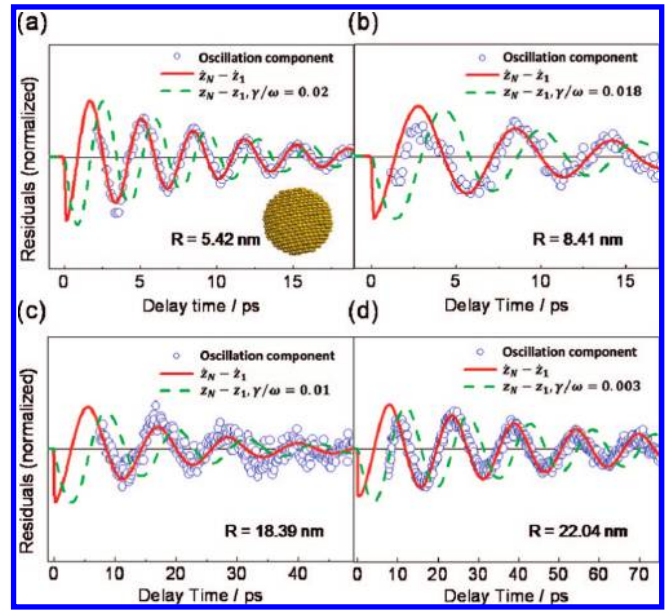

Figure 4. (a−d) The transient absorption profiles (open circle) of gold nanospheres with various radii, in comparison with simulations.

Twice the bisector represents the averaged distance for a sound wave to travel on the surface of a triangle. Such a size dependence on the oscillation period for a nanoprism has also been reported by others.[12,15,16] It is interesting to point out that the phase of the oscillations is better described by changes in the bisector height rather than its time derivative, as obtained for two previous thin-film examples. The cause of the 90° phase shift for such a mode in nanoprisms is unlikely due to laser fluence dependence, which is rather small. It could be due to how such an acoustic mode is excited and coupled to the SPR band. The details remain for future investigation. Observation of a 90° phase shift was also noticed in a recent study of silver nanocubes by Petrova et al.[30] They attributed the cause to

TABLE 2: Parameters for Different Nanomaterials with FPU−TTM Modeling

items	dimension (nm)	fitted length (nm)	FPU−TTM model	measured periods (ps)	oscillation periods
Au film	$T = 50.0$	$T = 48.1$ ($N = 168$)	$\dot{z}_N(t) - \dot{z}_1(t)$	29.5	$2T/v_S$
Ag film	$T = 23.0$	$T = 22.0$ ($N = 77$)	$\dot{z}_N(t) - \dot{z}_1(t)$	12.3	$2T/v_S$
Ag prism	$H = 31.4 \pm 8.5$	$H = 31.2$ ($N = 109$)	$z_N(t) - z_1(t)$	17.1	$2L/v_S$
	$T/2 = 4.3 \pm 0.4$	$T/2 = 5.2$ ($N = 19$)	$\dot{z}_N(t) - \dot{z}_1(t)$	3.25	T/v_S
	$T/2 = 3.9 \pm 0.6$	$T/2 = 4.3$ ($N = 16$)	$\dot{z}_N(t) - \dot{z}_1(t)$	2.85	T/v_S
Au sphere	$D/2 = 5.3 \pm 0.4$	$D/2 = 5.2$ ($N = 19$)	$\dot{z}_N(t) - \dot{z}_1(t)$	3.4	D/v_S
	$D/2 = 8.4 \pm 0.8$	$D/2 = 8.9$ ($N = 32$)		5.4	
	$D/2 = 15.6 \pm 2.1$	$D/2 = 18.1$ ($N = 64$)		11.1	
	$D/2 = 22.1 \pm 2.6$	$D/2 = 24.8$ ($N = 87$)		15.0	
Au rod	$L = 55.0 \pm 15.0$	$L = 68.8$ ($N = 240$)	$z_N(t) - z_1(t)$	62.0	$2L/v_E$
	$D/2 = 13.0 \pm 1.0$	$D/2 = 17.6$ ($N = 62$)	$\dot{z}_N(t) - \dot{z}_1(t)$	11.0	D/v_S
Au disk	$D = 88.0$	$D = 87.6$ ($N = 305$)	$z_N(t) - z_1(t)$	52.8	$2D/v_S$
Au triangular pyramid	$H = 104.0$	$H = 117.8$ ($N = 410$)	$z_N(t) - z_1(t)$	74.8	$2H/v_S$

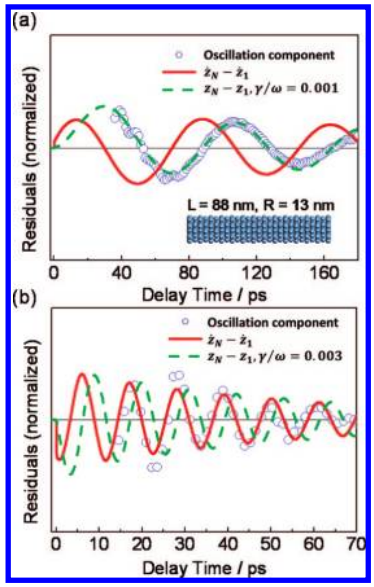

Figure 5. (a) The long-time slower oscillating components in transient absorption profile (open circle) for gold nanorods with a length $L = 55 \pm 15$ nm and a radius $R = 13 \pm 1$ nm. (b) The short-time faster oscillations due to wave propagation along the radius direction.

uniform and nonuniform strains. In another study,[12] the oscillations were fitted by two modes, with one mode along the bisector and the other along the side of a triangle. However, such a two-component fitting to low S/N data is not too reliable. Nevertheless, we do observe previously unnoticed fast oscillations at a very short time scale. These oscillations and model fitting for two different sizes are illustrated in Figure 3b and c. These fast oscillations correspond to sound wave propagation perpendicular to the triangle-shaped surface, and the period is given by the film thickness divided by the sound speed. The phase is 90° out of phase as compared to the other mode.

In the third example using our own experimental data of gold nanospheres at four sizes, the results are illustrated in Figure 4a−d. As thin films, the experimental data follows nicely $\dot{z}_N(t) - \dot{z}_1(t)$. The fitted oscillation period corresponds approximately to the diameter divided by the sound speed, which differs from the theoretical value by 10%.[16] In the fourth example, we considered gold nanorods and fitted the experimental data of Hu et al.[17] The signal appears to consist of two modes. One mode corresponds to the extensional mode along the cylindrical axis with a period given by twice the rod length divided by the sound speed v_E (1824 m/s) for the extensional mode. The speed for the extensional mode for a thin rod is known to be slower than the regular bulk sound speed, v_S (3240 m/s). The oscillations of such a mode can be best fitted using $z_N(t) - z_1(t)$. However, the other mode which describes sound wave propagation along the radial direction can be best fitted by $\dot{z}_N(t) - \dot{z}_1(t)$. In addition, the oscillation period is related to the diameter divided by the regular sound speed.

In the fifth example, we considered gold nanodisks with an orientation perpendicular to incident light. Using the experimental data of Huang et al.,[31] we obtained a good fit using $z_N(t) - z_1(t)$ with the oscillation period equal to twice the diameter divided by the sound speed. In comparison, for a sphere, the oscillation period is equal to twice the radius divided by the sound speed. In the last example, we analyzed the experimental data of a gold triangular pyramid measured by Huang et al.[15] The oscillation period is equal to twice the bisector height divided by the sound speed, and the temporal behavior can be best fitted by $z_N(t) - z_1(t)$. Such dependence is similar to those of nanoprisms.

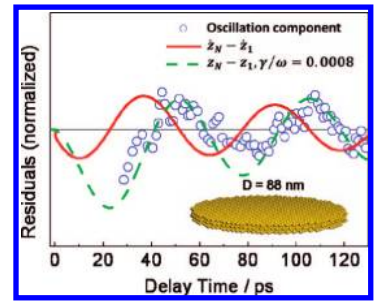

Figure 6. The deduced oscillating component (open circles) for gold nanodiscs with $D = 88$ nm and $T = 25$ nm in comparison with simulations.

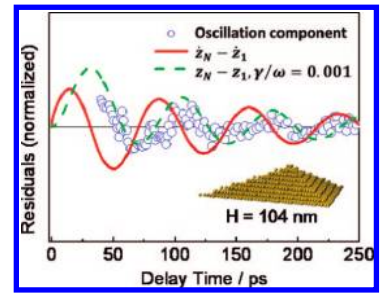

Figure 7. The deduced oscillating component (open circles) for gold triangular pyramids as compared with model simulations. The bisector height is 104 nm.

Conclusions

In this work, we have systematically examined photoinduced acoustic waves by transient optical absorption studies of metal nanomaterials. Experimental data of our own and those from others for six different shapes and various sizes of gold or silver composition were analyzed here. The fitted parameters and the relevant phase for the fits for these examples are listed in Table 2 for better comparison. From this Table, one can draw a conclusion about the phase for the acoustic wave excitation. For a thin film or a sphere, the observed excited acoustic mode is parallel to the incident light, and the observed amplitude is best described by $\dot{z}_N(t) - \dot{z}_1(t)$. In contrast, the mode for sound wave propagation along the cylindrical axis of a rod or along the prism or disk surface that is perpendicular to the incident light there is a 90° phase shift, and the observed amplitude is best described by $z_N(t) - z_1(t)$. For an ensemble sample of prisms, discs, pyramids, or rods in the experiments, most likely, the orientation of their major planar or cylindrical surfaces and the sound propagation of the observed mode are perpendicular to the incident light. In contrast, in thin films and spheres or the weaker mode in prisms (perpendicular to the triangle surface) or in cylinders (perpendicular to the cylindrical axis), the excited acoustic mode is parallel to the incident light. Briefly speaking, if the direction of expansion and contraction is along the direction of light propagation, the amplitude is best described by $\dot{z}_N(t) - \dot{z}_1(t)$. On the other hand, if the mode of acoustic wave is along the major dimension of nanoparticles with a large aspect ratio, such as a rod, prism, pyramid, and disk, the amplitude is best described by $z_N(t) - z_1(t)$. We have performed 2-D simulations for a prism and have found that the phase for the acoustic phonon mode along the direction of an impulse and the phase for the other mode with sound wave propagating perpendicular to the impulse indeed have a 90° phase shift. The FPU−TTM model provides a better physical picture than the usual phenomenological model, assuming a simple damped oscillator for the whole film or nanoparticle. We have uncovered an interesting phase shift for the photoinduced acoustic excita-

tion for some shapes and modes. Such a distinctive phase shift might be related to how these modes coupled to the SPR mode. Our model simulations offer reasonably good agreement with the observed nanoscale heat transfer and structural dynamics induced by femtosecond laser heating of nanosize thin films and prisms.

Acknowledgment. This work is supported by Academia Sinica and the National Science Council of Taiwan (No. 96-2113-M-001-032-MY3 for J.T.). J.T. benefited from helpful discussions with P. T. Tai.

References and Notes

(1) Patel, C. K. N.; Tam, A. C. *Rev. Mod. Phys.* **1981**, *53*, 517.
(2) Rentzepis, P. M.; Pao, R. H. *J. Chem. Phys.* **1966**, *44*, 2931.
(3) Fujimoto, J. G.; Liu, J. M.; Ippen, E. P.; Bloembergen, N. *Phys. Rev. Lett.* **1984**, *53*, 1837.
(4) Eesley, G. L. *Phys. Rev. B* **1986**, *33*, 2144.
(5) Thomsen, C.; Grahn, H. T.; Maris, H. J.; Tauc, J. *Phys. Rev. B* **1986**, *34*, 4129.
(6) Brorson, S. D.; Fujimoto, J. G.; Ippen, E. P. *Phys. Rev. Lett.* **1987**, *59*, 1962.
(7) Wright, O. B.; Kawashima, K. *Phys. Rev. Lett.* **1992**, *69*, 1668.
(8) Sun, C.-K.; Vallée, F.; Acioli, L.; Ippen, E. P.; Fujimoto, J. G. *Phys. Rev. B* **1993**, *48*, 12365.
(9) Hohlfeld, J.; Müller, J. G.; Wellershoff, S.-S.; Matthias, E. *Appl. Phys. B: Laser Opt.* **1997**, *64*, 387.
(10) Hartland, G. V. *Annu. Rev. Phys. Chem.* **2006**, *57*, 403.
(11) Hartland, G. V. *J. Chem. Phys.* **2002**, *116*, 8048.
(12) Bonacina, L.; Callegari, A.; Bonati, C.; van Mourik, F.; Chergui, M. *Nano Lett.* **2006**, *6*, 7.
(13) Wang, J.; Guo, C. *Phys. Rev. B* **2007**, *75*, 184304.
(14) Del Fatti, N.; Voisin, C.; Christofilos, D.; Vallée, F.; Flytzanis, C. *J. Phys. Chem. A* **2000**, *104*, 4321.
(15) (a) Huang, W.; Qian, W.; El-Sayed, M. A. *Nano Lett.* **2004**, *4*, 1741. (b) Huang, W.; Qian, W.; El-Sayed, M. A. *J. Phys. Chem. B* **2005**, *109*, 18881.
(16) Hu, M.; Petrova, H.; Wang, X.; Hartland, G. V. *J. Phys. Chem. B* **2005**, *109*, 14426.
(17) Hu, M.; Wang, X.; Hartland, G. V.; Mulvaney, P.; Juste, J. P.; Sader, J. E. *J. Am. Chem. Soc.* **2003**, *125*, 14925.
(18) Cavalleri1, A.; Siders, C. W.; Brown, F. L. H.; Leitner, D. M.; Tóth, C.; Squier, J. A.; Barty, C. P. J.; Wilson, K. R.; Sokolowski-Tinten, K.; Horn von Hoegen, M.; von der Linde, D.; Kammler, M. *Phys. Rev. Lett.* **2000**, *85*, 586.
(19) Lindenberg, A. M.; Kang, I.; Johnson, S. L.; Missalla, T.; Heimann, P. A.; Chang, Z.; Larsson, J.; Bucksbaum, P. H.; Kapteyn, H. C.; Padmore, H. A.; Lee, R. W.; Wark, J. S.; Falcone, R. W. *Phys. Rev. Lett.* **2000**, *84*, 111.
(20) Park, H.; Wang, X.; Nie, S.; Clinite, R.; Cao, J. *Phys. Rev. B* **2005**, *72*, 100301.
(21) Tang, J. *Appl. Phys. Lett.* **2008**, *92*, 011901; Tang, J. *J. Chem. Phys.* **2008**, *128*, 164702.
(22) Jiang, L.; Tsai, H.-L. *J. Heat Transfer* **2005**, *127*, 1167.
(23) Valette, S.; Harzic, R. L.; Huot, N.; Audouard, E.; Fortunier, R. *Appl. Surf. Sci.* **2005**, *247*, 238.
(24) Wright, O. B. *Phys. Rev. B* **1994**, *49*, 9985.
(25) Perner, M.; Gresillon, S.; März, J.; von Plessen, G.; Feldmann, J.; Porstendorfer, J.; Berg, K.-J.; Berg, G. *Phys. Rev. Lett.* **2000**, *85*, 792.
(26) Achcroft, N. W.; Mermin, N. D. *Solid State Physics*; Saunders College Press: Philadelpha, 1976.
(27) Kriebig, U.; Vollmer, M. *Optical Properties of Metal Clusters*; Springer Press: New York, 1995.
(28) Groeneveld, H. M. R.; Sprik, R.; Lagendijk, A. *Phys. Rev. B* **1995**, *51*, 11433.
(29) Atkins, P. W. *Physical Chemistry*; Oxford University Press: New York, 2002.
(30) Petrova, H.; Lin, C.-H.; de Liejer, S.; Hu, M.; McLellan, J. M.; Siekkinen, A. R.; Wiley, B. J. *J. Chem. Phys.* **2007**, *126*, 094709.
(31) Huang, W.; Qian, W.; Jain, P. K.; El-Sayed, M. A. *Nano Lett.* **2007**, *7*, 3227.

JP806498Y